

## Fractal Vicsek MIMO Antenna for LTE and 5G Applications

**Abstract.** A Vicsek MIMO antenna was designed in the band of 3.3 – 4.99 GHz for both LTE and 5G communications is demonstrated in this paper. The proposed antenna is printed on a FR-4 substrate material and dimension of the antenna was  $24 \times 46 \times 0.8 \text{ mm}^3$ . This paper presents the development of a compact MIMO antenna using a new structure integrated with the Vicsek using neutralization line and defected ground structure techniques for mutual coupling (MC) reduction and antenna isolation improvement. The simulated results proved that the proposed method gives an excellent isolation performance. A good impedance matching return loss of large than 10 dB, high isolation of large than 16.5 dB at the operating frequency, and low envelope correlation coefficient (ECC) that was 0.0035 was simulated across the coveted operating bandwidth.

**Streszczenie.** W tym artykule zademonstrowano antenę Vicsek MIMO o paśmie 3,3 – 4,99 GHz dla komunikacji LTE i 5G. Proponowana antena jest wydrukowana na materiale podłoża FR-4, a jej wymiary to  $24 \times 46 \times 0,8 \text{ mm}^3$ . W artykule przedstawiono opracowanie kompaktowej anteny MIMO z wykorzystaniem nowej struktury zintegrowanej z anteną Vicsek przy użyciu techniki linii neutralizacyjnej i uszkodzonej struktury gruntu w celu redukcji wzajemnego sprzężenia (MC) i poprawy izolacji anteny. Wyniki symulacji wykazały, że proponowana metoda zapewnia doskonałą wydajność izolacji. Zasymlulowano dobrą stratę powrotną dopasowującą impedancję większą niż 10 dB, wysoką izolację większą niż 16,5 dB przy częstotliwości roboczej oraz niski współczynnik korelacji obwiedni (ECC), który wynosił 0,0035 w całej pożądanej szerokości pasma. (Antena Fractal Vicsek MIMO do zastosowań LTE i 5G)

**Keywords:** MIMO antenna, mutual coupling, Fractal, Vicsek, Isolation, 5G.  
**Słowa kluczowe:** antena MIMO, antena Vicsek, fractal, LTE

### Introduction

Over 40 years, four generations of wireless mobile phones evolution have been synchronous the technological advancement of hand-held cellular device. At 1990s, elimination of mobile phones antenna was realized, result in revolution of different mobile models with establishing a new wireless service, creation of the cellular advances of the current cycle and advances in technologies of mobile antennas[1].

This revolution triggered increased wireless traffic continuous demands leading to the introduction of the fifth generation (5G) which is the policy makers and wireless engineers interesting pivotal. The 5G wireless network should be supplied by OFDM, GSM, UMTS and CDMA2000, UWB and IPv6, 4G and 5G are running on last one. Because of such basic protocol depending on location management with assigning IP addresses to mobile nodes, 5G is depending on network access management with it is design that is concerned from worldwide wireless web to mobile devices that lead to waste in resources of such wireless networks, meanwhile it is hard to run IPv6 on which 5G depend [2]–[4]

To address such incompatibility problem, a Bandwidth Optimization Control Protocol (BOCP) is proposed and emerge the 5G data path bandwidth. BOCP has implemented between the TCP/IP and MAC layers which roll in bandwidth mix. It is worth to mention, the spectrum of 5G has been classified into two frequency bands of sub-6 GHz and mm-waves. The first one is customizing for the service of citizen radio broadband which is around 3.5 GHz that used the platform structure of 4G Long Term Evolution (LTE)[5], [6], while the second band is above 24 GHz which was approved unanimously by the Federal U.S. Communications Commission (FCC) in June 2016.

In order to pave the way to 5G services of mm waves that comprises of unlicensed and shares spectra. In order to maximize spectrum usage, lots of effort has been directed towards combining and integrating the unlicensed, licensed and shared spectra[3]. However, utilization of microwave frequencies from 3.1 to 10.5 GHz faces challenges related to a number of antennas used which in turn affects the configuration of currently mobile antenna. Meanwhile, spectrum situation of mm-Waves is uncertain and more

complicated. The community of wireless lacking knowledge and experiences of how to dedicate mm radio waves to mobile phones. That exacerbate the situation of strongly entire relation between phone design and major antennas. Besides, the design of multiple-input multiple-output antennas covering a limited space demands different methods for the increasing of isolation between ports of MIMO antenna, differently, radiation patterns, efficiency, the gain (G), diversity gain(DG) and envelope correlation coefficient (ECC) would be affected. Thus, the mutual coupling reduction techniques should be applied with greater care, and other parameters must be considered. One of the possible solutions to the problem of mutual coupling (MC) is the use of isolation techniques. The isolation decreases between antenna elements and improves the ECC, DG, G and efficiency of the system High gain antenna at 915 mhz for off grid wireless networks[2]–[4], [7]. As such, this paper attempted to explain the above-mentioned issues with low MC printed on FR-4 material which covers a centre frequency of 4.2 GHz in the band of 3.3-4.99 GHz.

### Antenna Design and Analysis

The concept of fractals, plays an important role in characterization of the features in complex systems, in nature, since many objects in the real world can be modelled by fractals. Hence, a fractal is a pattern that repeats itself at smaller scales, resulting in an irregular shape. The geometry of the elliptical-shaped patch with slot vicsek is shown in Figure 1(c). The dimensions of fundamental design parameters for the elliptical structure included radii of 11 mm and of 6 mm. The structure was made by FR4 substrate with relative permittivity of  $\epsilon_r = 4.3$  and thickness of  $ht = 0.08 \text{ mm}$ . The cell of the proposed design was a circular antenna with the process undertaken in three stages. In the first stage, a circular shape antenna (antenna 1) with a radius of 8.125 mm was designed. Figure 1(a) illustrates the first stage comprising circular antenna design. The radius (r) of the circular antenna was calculated using Equation (1) [8], [9]:

$$(1) \quad r = \frac{F}{\sqrt{1 + \left(\frac{2h}{\pi\epsilon_r F}\right) \left[\ln\left(\frac{\pi F}{2h}\right) + 1.7226\right]}}$$

where  $r$  is the radius of the circular antenna while  $F$  is given by Equation (2) [8]:

$$(2) \quad F = \frac{8.791 \cdot 10^9}{f_r \cdot \sqrt{\epsilon_r}} \quad )$$

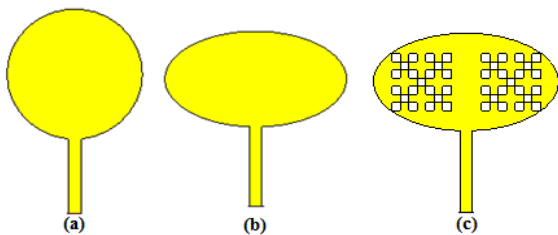


Fig. 1: Configuration Process of the viscek Antenna (a) Stage1 Circular Antenna (b) Stage 2 Elliptical Antenna (c) Stage 3 viscek Antenna

In the second stage, the circular shape antenna was modified to an elliptical antenna (antenna 2) using two radii (11 mm and 6 mm in dimensions). Figure 1(b) shows the patch antenna of stage 2. An enhancement of the circular patch (antenna 1) to an elliptical patch (antenna 2) was done according to Equations (3) – (6). The lower frequency of the bandwidth was determined by making the size of the planar configuration equal to the size of cylindrical wire with a height of  $l$  mm, which is equal to the height of the planar disc. While the radius ( $r$ ) is calculated using Equation (4)[10]:

$$(3) \quad \pi \cdot r^2 = \pi \cdot a \cdot b$$

The antenna length for the real input impedance was determined by Equation (5) below [10]:

$$(4) \quad l = 0.24 \cdot \lambda \cdot F$$

and

$$(5) \quad F = \frac{l/r}{(1+l/r)}$$

From Equations (3) – (5), a resonant frequency can be determined as given in Equation (6):

$$(6) \quad f_r = \frac{c}{\lambda} = \frac{3 \cdot 10^8 \cdot 0.24}{(1+r)}$$

$$\text{Let } \frac{0.24}{(1+r)} = Q$$

$$(7) \quad f_r = \frac{c}{Q \cdot \sqrt{\epsilon_r}}$$

In the third stage, the viscek antenna (antenna 3) was designed fractal viscek slot on the patch plane in the final stage. In general, the geometry of fractal shape starts with a square in 0th iteration as shown in Figure 2 (a). In 1st iteration, the square was divided into four small squares of equal sized located at the four corners as shown in Figure 2 (b). In 2nd iteration, five squares were further divided into twenty five small equal sized squares and moved to the four corners as shown in Figure 2 (c). In 3rd iteration, twenty-five squares were divided into one hundred small equal sized squares and moved to the four corners as shown in Figure 2 (d). If the iterative process is continued, an unlimited number of squares will be obtained to form an ideal fractal geometry called viscek-shaped. The shape of viscek will be having limited the size.

The linear dimensions of the fractal slot were determined to design the fractal perimeter along the boundary of the square fractal slot. The length of  $L$  was equal to the horizontal and vertical sides of the square, where  $L = X = Y$ . The iterations can be analyzed by calculating the number of squares in Figure 2. The number of squares in 0th Iteration is 1. The total number of squares in 1st iteration is  $5 \times 5 = 25$ . Also, the total number of squares in 3rd iteration is  $5 \times 5 \times 5 = 125$  square, and Equation (8) can be used to calculate the number of squares:

(8) Number of squares =  $5^i$  where,  $i = 0, 1, 2, 3, 4, \dots$

The next step was to calculate the length square of the iterations. In 0th iteration, the dimension of the original square started with  $L$  mm. Table 1 displays relationship between the length of squares and the number of squares. The length square for the 1st iteration was  $L/3$ . Then, the length of a square for 2nd iteration was  $L/9$  mm and for 3rd iteration was  $L/27$ . Equation (9) can be used to calculate the length square of the iterations:

$$(9) \quad \text{length square of the iterations} = \frac{L^i}{3^i}$$

where,  $i = 0, 1, 2, 3, 4, 5 \dots$

Table 1: Relationship Between Number of Squares and length of Squares

Iteration	Length of Square's Side (mm)	Number of Squares
0	$L$	$5^0 = 1$
1	$L/3$	$5^1 = 5$
2	$L/(3 \times 3)$	$5^2 = 25$
3	$L/(3 \times 3 \times 3)$	$5^3 = 125$

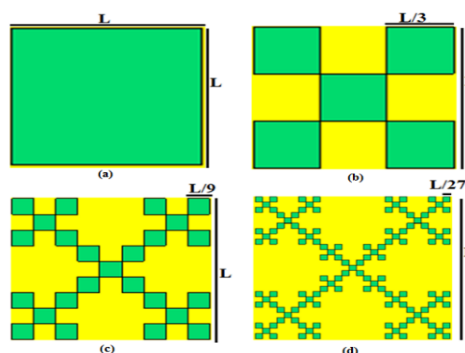


Fig. 2: Configuration Process of the Viscek Antenna (a) 0th iteration (b) 1st Iteration (c) 2nd Iteration (d) 3rd Iteration

In this design, The geometry of fractal shape starts with a square in 0th iteration as shown in Figure 3 (a). In 1st iteration, the square was divided into four small squares of equal sized located at the four corners as shown in Figure 3 (b). In 2nd iteration, five squares were further divided into twenty-one small equal-sized squares and moved to the four corners with a shift of one square for every corner as shown in Figure 3 (c). In 3rd iteration, twenty-one squares were divided into one hundred small equal sized squares and moved to the four corners with a shift of one square for every corner as shown in Figure 3 (d). Table 2 displays relationship between the length of squares and the number of squares. Equations (10) - (12) can be used to calculate the number of squares and length of sequers:

$$(10) \quad \text{Number of squares} = 5^i \quad \text{where, } i = 0, 1$$

$$(11) \quad \text{Number of squares} = [\text{last iteration} \cdot 5] - 4$$

where,  $i = 2, 3, 4, 5, \dots$

$$(12) \quad \text{length of side square} = \frac{L}{[\text{last iteration} \cdot 3] - 2}$$

$i = 0, 1, 2, 3, 4, 5 \dots$

Table 2 Relationship Between Number of Squares and length of Squares

Iteration	Length of Square's Side (mm)	Number of Squares
0	$L$	$5^0 = 1$
1	$L/3$	$5^1 = 5$
2	$L/(3 \cdot 3 - 2) = L/7$	$5^2 \cdot 5 - 4 = 21$
3	$L/(7 \cdot 3 - 2) = L/19$	$21 \cdot 5 - 4 = 101$

The cell geometry of the suggested MIMO antenna is shown in Figure 4. The cell dimensions of antenna were to be  $L_f = 10.013$  mm,  $W_f = 1.47$  mm,  $W_t = 24$  mm and  $L_t =$

46 mm. In order to obtain high isolation, DGS technique was designed by cutting a slot having a length of  $L4 = 1$  mm and width  $g4 = 2$  mm, with adding another slot having the length of  $L5 = 1$  mm and width  $g3 = 1$  mm in the ground plane. However, the NLS was designed by adding two lines in the patch plane, the first is vertical line with length of 24 mm and length  $L3 = 1.5$  mm. The second is horizontal line of width (length vertical line -  $L1 - L2 = 1$  mm) and length = 2.077 mm. The suggested techniques were configured by combining DGS and NLs. The configuration process for the two techniques is shown in Figure 4. The dimensions of the proposed MIMO antenna are mentioned in Table 3. Radiating elements of the two-element MIMO antenna design have asymmetric monopole antenna, fed by a 50  $\Omega$  microstrip line. In Figure 4, The proposed MIMO antenna proposed includes two separate ports with a distance less than  $0.5\lambda = 2.077$  mm, monopoles printed on a  $24 \times 46$  mm FR-4 substrate with a dielectric constant of 4.3 with a thickness of 0.8 mm.

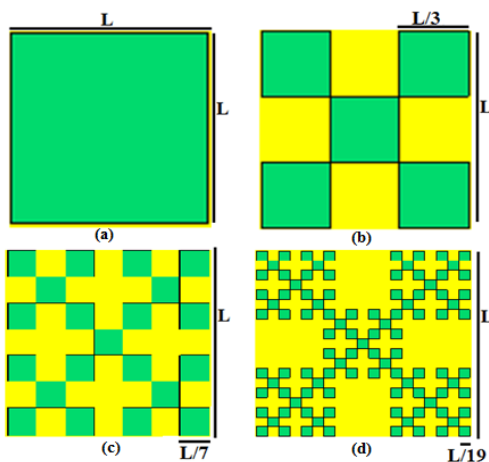


Fig. 3: Configuration Process of the Viscek Antenna (a) Square 0th Iteration (b) Square 1st Iteration (c) Square 2nd Iteration (d) Square 3rd Iteration

Table 3: Dimensions (mm) of the Parameters of vicsek MIMO Antenna

Parameters	L1	L2	L3	L4	L5	L6
Dimensions	15.5	7.5	1.5	1	1	0.5
Parameters	L7	g1	g2	g3	g4	g5
Dimensions	0.75	5.831	5	5	2	1
Parameters	g6	g7	R1	R2	Wt	Lt
Dimensions	4.665	5	11	6	24	46
Parameters	Wf	Lf	ht	hs	-	-
Dimensions	1.47	10.013	0.0035	0.8	-	-

### Performances MIMO antenna

The simulated reflection coefficients ( $S_{11}$ ) and the fractal antenna isolations ( $s_{12}$ ) are shown in Figure 5 of design. The fractal antenna has shown a good response within the chosen frequency band. The simulated impedance bandwidth shows good coverage around the centre frequency of 4.2 GHz. Also, a significant shift in  $S_{11}$  is given at a distance of 2.077 mm due to high coupling between the two-element. In this paper, the main focus is to increase isolation between dual-element MIMO at the wanted band. From these results, the optimum fractal MIMO antenna in this work has been selected at 2.077 mm distance between dual-element due to its overall performance for both LTE and 5G MIMO application.

To obtain high isolation, NL was inserted between the two separated antenna elements and DGS slots were inserted on the ground plane. The NL used two vertical lines on the ground plane and patch plane. However, the

DGS technique was designed by cutting a slot having a length of  $L4 = 1$  mm and width  $g4 = 2$  mm, with adding another slot having the length of  $L5 = 1$  mm and width  $g3 = 1$  mm in the ground plane. In addition, the parametric study showed that the frequency response and bandwidth of the MIMO antenna are greatly influenced by slots width on the ground plane. An increase or decrease in the width of these slots was found to have induced a change in the centre resonant frequency of the design bandwidth. As can be observed from Figure 6, the isolation technique significantly increased the isolation between the antenna elements, by a significant reduction in the  $S_{12}$  curve. Two Isolation techniques (NL and DGS) were used in the proposed antenna. The hybrid technique reduced the coupling in the ground plane and, increased isolation between the antenna elements. Adding to that, the antennas were placed horizontal, 2.077 mm apart, which further enhances the isolation between the antenna elements.

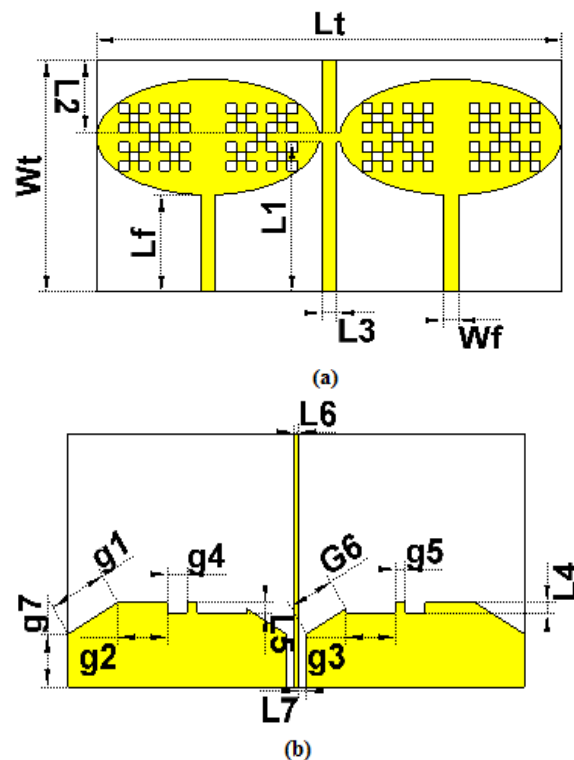


Fig. 4 Geometry of the Proposed vicsek MIMO Antenna (a) Front View (b) Back View

A maximum envelope correlation coefficients (ECC) obtained was 0.0035 for the band (3.3 - 4.99) GHz for both LTE and 5G applications, as shown in Fig. 7. In addition, A good level of efficiency 89-93% was obtained from the respective operating band, and the efficiency of the proposed MIMO antenna was above 89% in the operating band, as shown in Fig.8. Diversity gain (DG) is another important factor that must be taken into account while evaluating the performance of MIMO antenna system. It provides information about the reliability of the MIMO system. The higher value of diversity gain signifies better isolation between antenna elements. It depends on the correlation coefficients between antenna signals is given by the following Equation[11]:

$$(13) \quad DG = 10 \sqrt{1 - |ECC|^2}$$

Figure 9 shows the diversity gain of the proposed design, observed that the suggested MIMO antenna provides high  $DG > 9.985$ .

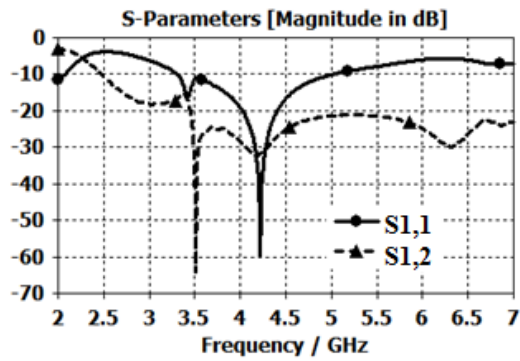


Fig. 5: S-Parameters of the vicsek MIMO antenna

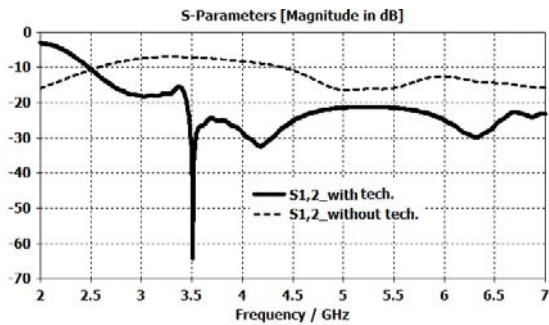


Fig. 6: Isolation with and without techniques

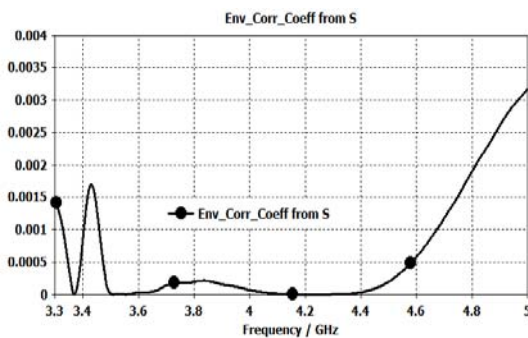


Fig. 7: Simulated ECC of the vicsek MIMO Antenna of Band (3.3-4.99) GHz

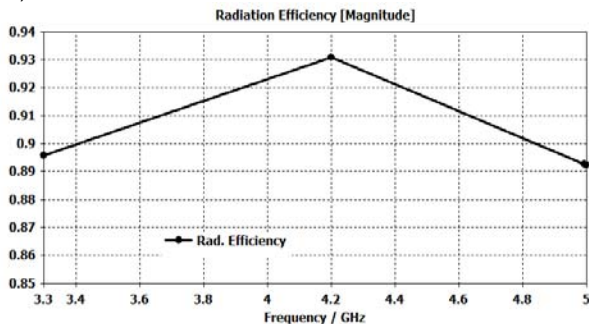


Fig. 8: Efficiency of the vicsek MIMO antenna

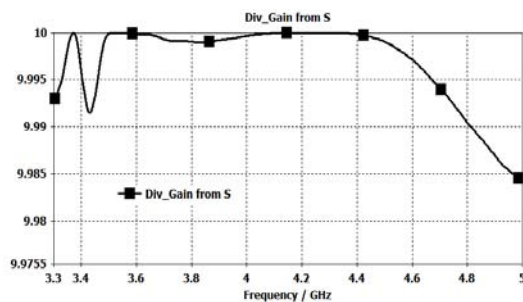


Fig. 9: DG of Vicsek MIMO Antenna

As shown in Figure 10, the current in the input element was taken at a specific location where the impedance was minimum and the current was maximum, and then its phase was reversed by the hybrid isolation technique. This reverse current was then fed to the nearby antenna to reduce the amount of coupled current. The mutual coupling problem between the two antennas was solved by the NL method. From the surface current distribution in Figure 10, it can be observed that the current is mainly concentrated around the slots, which generates inverse surface current and thus, reduces the coupling between the antenna elements.

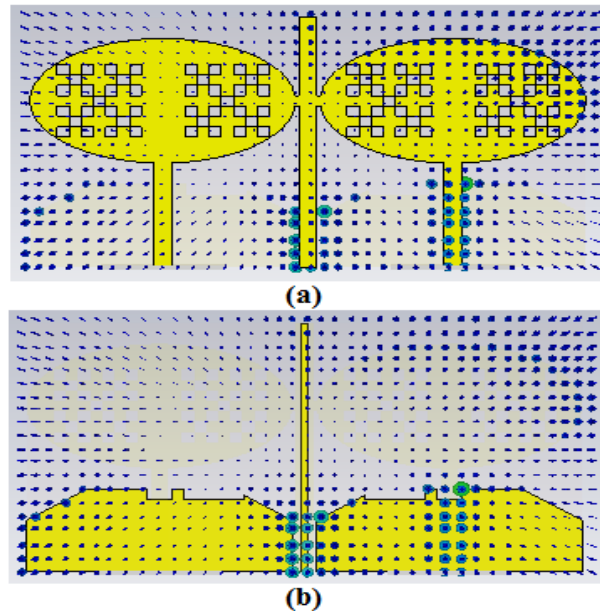


Fig. 10: Simulated current densities with port1 of the fractal vicsek MIMO antenna (a) Patch patch plane (b) Ground plane

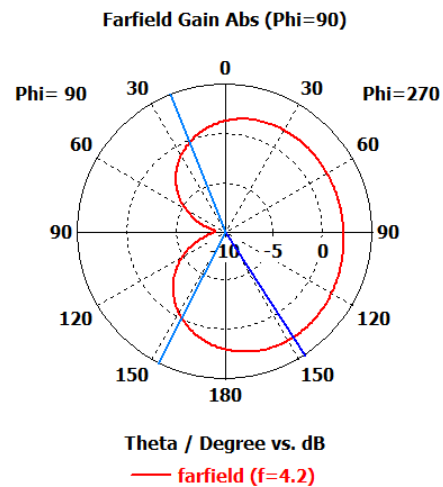


Fig. 11: Radiation Characteristics of proposed antenna at centre frequency 4.2 GHz.

Figure 11 shows the simulated radiation pattern of the proposed MIMO antenna for a centre frequency of 4.2 GHz when Port 1 is excited.

The antenna prototypes were fabricated for the 3.3-4.99 GHz band with an operating frequency of centre 4.2 GHz, from an inexpensive FR-4 dielectric and with overall dimensions of  $24 \times 46 \times 0.8 \text{ mm}^3$ , as shown in Figure 12. The simulated and measured reflection and transmission coefficients, demonstrated by the two representative antennas, were implied to have a similar level of performance, the antenna prototypes have shown measured isolation 16.5 dB at operating frequency band, as shown in Figure 13.

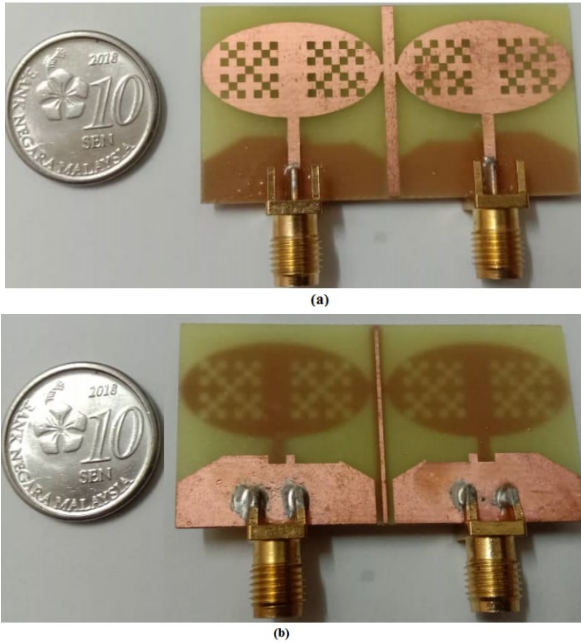


Fig. 12: A photograph of the Fabricated Fractal vicsek MIMO Antenna (a) Patch plane (b) Ground plane

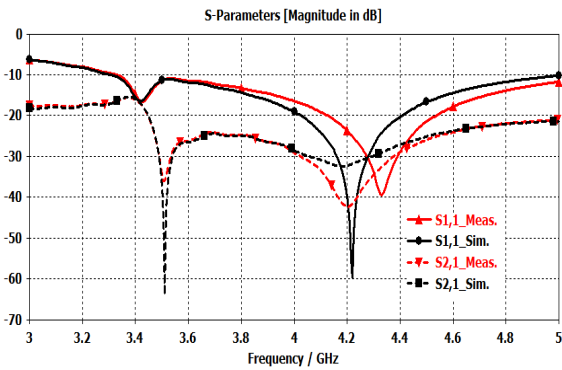


Figure 13: The Simulated and Measured S-Parameters

### Validation of the Proposed Antenna

Table 1 shows, the comparison of findings between this research works with other research work. The proposed antenna is compared with several selected types of research. The comparison was based on important characteristics, such as several ports, isolation, efficiency, envelope correlation coefficient, material, bandwidth and size. This vicsek MIMO antenna is the best for LTE and 5G communications propose for several reasons.

Table 1: Comparisons between the proposed of MIMO antennas and previous related antennas

Ref.	BW (GHz),	Size (mm <sup>3</sup> )	Iso.	ECC
[12]	(2.4–2.48)	60 × 7.5 × 4.5	16	< 0.015
[13]	(3.4–3.8)	60 × 25 × 1.6	14	< 0.015
[14]	(3.3–3.6)	43 × 26 × 0.8	18	< 0.1
[15]	(3.4–4.7)	26 × 46 × 0.8	12	< 0.008
[16]	(3.9–4.2)	40.5×40.5×1.6	17	< 0.035
[17]	(3.6–3.99)	37 × 56 × 1.6	-10	< 0.08
[18]	(3.47–3.58)	40 × 40 × 2.5	18.5	< 0.04
This work	(3.3-4.99)	24 × 46 × 0.8	16.5	< 0.003

### Conclusion

A mobile phone with a two-element antenna design was proposed for the use of LTE and 5G MIMO communications. This job involved the simulation of a novel fractal MIMO antenna for the band range of (3.3-4.99)

GHz. The isolation was increased by way of the application of decoupling hybrid technique (neutralization lines and defected ground structure). Besides enhancing the isolation between the antenna elements, the ECC between the signals received by the MIMO antenna ports was sufficiently reduced to meet the specifications for both LTE and 5G applications.

**Authors:** Noora Rafid Kamil, Email: noorarafid1994@gmail.com; Aseel Hameed Majeed, Email: aseel\_alnakkash@mtu.du.iq Ahmed Ghanim Wadday, Email: ahmadghw@atu.edu.iq; Ayman Dheyaa Khaleel, Email: aymendheyaa@yahoo.com.

### REFERENCES

- [1] E. AIMousa and F. AlShahwan, "Performance Enhancement in 5G Mobile Network Processing," *Lect. Notes Inf. Theory*, 2015, vol. 3, no. 1, pp. 19–24.
- [2] A. K. Jain, R. Acharya, S. Jakhar, and T. Mishra, "Fifth Generation (5G) Wireless Technology 'Revolution in Telecommunication,'" *Proc. Int. Conf. Inven. Commun. Comput. Technol. ICICCT*, 2018, no. 9, pp. 1867–1872.
- [3] A. J. A. Al-Gburi et al., "High Gain of UWB CPW-fed mercedes-shaped printed monopole antennas for UWB applications," *Prz. Elektrotechniczny*, 2021, vol. 97, no. 5, pp. 70–73.
- [4] A. M. Ibrahim, I. M. Ibrahim, and N. A. Shairi, "Review isolation techniques of the MIMO antennas for Sub-6," *Prz. Elektrotechniczny*, 2021, vol. 97, no. 1, pp. 3–9.
- [5] M. Y. Zeain et al., "Design of a wideband strip helical antenna for 5g applications," *Bull. Electr. Eng. Informatics*, 2020, vol. 9, no. 5, pp. 1958–1963.
- [6] A. M. Ibrahim, I. M. Ibrahim, and N. A. Shairi, "Compact Crescent Slot MIMO Antenna with Quad Bands and High Isolation for LTE and 5G communications," *Prz. Elektrotechniczny*, 2020, no. 12, pp. 19–25.
- [7] H. H. Keriee et al., "High gain antenna at 915 mhz for off grid wireless networks," *Bull. Electr. Eng. Informatics*, 2020, vol. 9, no. 6, pp. 2449–2454.
- [8] C. A. Balanis, "ANTENNA THEORY ANALYSIS AND DESIGN," John Wiley, 2016.
- [9] A. H. Mousa, M. Azlishah, B. I. N. Othman, M. Z. Abidin, and A. M. Ibrahim, "Fractal H-Vicsek MIMO Antenna for 5G Communications," *Prz. Elektrotechniczny*, 2021, no. 6, pp. 15–20.
- [3] A. H. Mousa, M. Azlishah, B. I. N. Othman, M. Z. Abidin, and A. M. Ibrahim, "Sierpinski MIMO Antenna for 5G Applications," *Prz. Elektrotechniczny*, 2021, no. 7, pp. 126–131.
- [10] N. P. Agrawal, G. Kumar, and K. P. Ray, "Wide-band Planar Monopole Antennas - Antennas and Propagation," *IEEE Transactions on*, 1998, vol. 46, no. 2, pp. 294–295.
- [11] S. Chouhan, "Multiport MIMO antennas with mutual coupling reduction techniques for modern wireless transceive operations: A review," *RF Microw. Comput. -AIDED Eng.*, 2017, no. August, pp. 1–13.
- [12] J.-H. Chou, J.-F. Chang, D.-B. Lin, and T.-L. Wu, "Dual-band WLAN MIMO antenna with a decoupling element for full-metallic bottom cover tablet computer applications," *Microw. Opt. Technol. Lett.*, 2018, vol. 60, no. 5, pp. 1245–1251.
- [13] H. S. Singh, Shalini, and M. K. Meshram, "Printed Monopole Diversity Antenna for USB Dongle Applications," *Wirel. Pers. Commun.*, pp. 294–295., vol. 86, no. 2, pp.771–787.
- [14] A. K. Panda, S. Sahu, and R. K. Mishra, "A compact dual-band 2 × 1 metamaterial inspired mimo antenna system with high port isolation for LTE and WiMax applications," *Int. J. RF Microw. Comput. Eng.*, 2017, no. April, pp. 1–11..
- [15] A. M. Ibrahim, I. M. Ibrahim, and N. A. Shairi, "Compact MIMO antenna with high isolation for 5G smartphone applications," *J. Eng. Sci. Technol. Rev.*, 2019, vol. 12, no. 6, pp. 121–125.
- [16] I. Suriya and R. Anbazhagan, "Inverted-A based UWB MIMO antenna with triple-band notch and improved isolation for WBAN applications," *Int. J. Electron. Commun. ( AEU )*, 2019, vol. 99, pp. 25–33.
- [17] S. Chouhan, V. S. Kushwah, D. K. Panda, and S. Singhal, "Spider-shaped fractal MIMO antenna for WLAN/WiMAX/Wi-Fi/Bluetooth/C-band applications," *AEU - Int. J. Electron. Commun.*, 2019, vol. 110, p. 152871.
- [18] B. Niu and J. Tan, "Compact self-isolated MIMO antenna system based on quarter-mode SIW cavity," *Electron. Lett.*, 2019, vol. 55, no. 10, pp. 5–6.